



HHS Public Access

Author manuscript

Psychiatry Res Neuroimaging. Author manuscript; available in PMC 2021 May 30.

Published in final edited form as:

Psychiatry Res Neuroimaging. 2020 May 30; 299: 111064. doi:10.1016/j.psychresns.2020.111064.

Graph theoretical measures of the uncinate fasciculus subnetwork as predictors and correlates of treatment response in a transdiagnostic psychiatric cohort.

Paul J. Thomas^{a,b}, Srinivas Panchamukhi^a, Joshua Nathan, MD^c, Jennifer Francis, PhD^d, Scott Langenecker, PhD^e, Stephanie Gorka, PhD^a, Alex Leow, MD, PhD^{a,b}, Heide Klumpp, PhD^a, K. Luan Phan, MD^a, Olusola A. Ajilore, MD, PhD^{a,*}

^aDepartment of Psychiatry, University of Illinois at Chicago, Chicago, IL, USA

^bDepartment of Bioengineering, University of Illinois at Chicago, Chicago, IL, USA

^cLake County Health Department, Waukeegan, IL, USA

^dDepartment of Behavioral Sciences, Rush University, Chicago, IL, USA

^eDepartment of Psychiatry, University of Utah, UT, USA

Abstract

The internalizing psychopathologies (IP) are a highly prevalent group of disorders for which little data exists to guide treatment selection. We examine whether graph theoretical metrics from white matter connectomes may serve as biomarkers of disease and predictors of treatment response. We focus on the uncinate fasciculus subnetwork, which has been previously implicated in these disorders. We compared baseline graph measures from a transdiagnostic IP cohort with controls. Patients were randomized to either SSRI or cognitive behavioral therapy and we determined if graph theory metrics change following treatment, and whether these changes correlated with treatment response. Lastly, we investigated whether baseline metrics correlated with treatment response. Several baseline nodal graph metrics differed at baseline. Of note, right amygdala betweenness centrality was increased in patients relative to controls. In addition, white matter integrity of the uncinate fasciculus was decreased at baseline in patients versus controls. The SSRI and CBT cohorts had increased left frontal superior orbital betweenness centrality and left frontal

*Correspondence to: Olusola Ajilore, Department of Psychiatry, University of Illinois at Chicago, 1601 W Taylor St. Chicago, IL, 60612. oajilore@uic.edu; Phone: (312) 413-4562.

Author contributions.

Author PJT conducted preprocessing and reconstruction of MRI data and graph theoretical and statistical analyses. PJT also wrote the manuscript. Author SP conducted fractional anisotropy analyses. Authors JN and JF administered treatments to study participants. Authors HK, SG and AL advised on statistical analysis and manuscript edits. Authors SL, KLP and OAA designed the study and wrote the protocol. All authors contributed to and have approved the final manuscript.

Publisher's Disclaimer: This is a PDF file of an unedited manuscript that has been accepted for publication. As a service to our customers we are providing this early version of the manuscript. The manuscript will undergo copyediting, typesetting, and review of the resulting proof before it is published in its final form. Please note that during the production process errors may be discovered which could affect the content, and all legal disclaimers that apply to the journal pertain.

Conflicts of interest

Olusola Ajilore and Alex Leow are co-founders of KeyWise AI. Alex Leow serves on the scientific advisory board of Buoy Health, Olusola Ajilore serves on the advisory board of Embodied Labs and Blueprint.

Declarations of competing interest

None

medial orbital clustering coefficient, respectively, suggesting the presence of treatment specific neural correlates of treatment response. This study provides insight on shared white matter network features of IPs and elucidates potential biomarkers of treatment response that may be modality-specific.

Keywords

Diffusion tensor imaging; Connectome; White matter; Depression; Anxiety; Network

1. Introduction

Internalizing psychopathologies (IPs) are characterized by disordered emotion processing (Kovacs & Devlin, 1998), and encompass a combined prevalence of at least 20% in the US (Kessler et al., 2005). Diseases that fall in this category are often comorbid with each other and include major depressive disorder (MDD), generalized anxiety disorder (GAD) and other related diagnoses (Kessler et al., 2005). A significant commonality uniting the IPs are their treatments: cognitive behavioral therapy (CBT) and selective serotonin reuptake inhibitors (SSRIs) are therapeutic mainstays across the swath of these disorders. While either treatment modality is generally effective for the majority of patients, most are started on SSRIs with a response rate of 50–70% for MDD or anxiety disorders (Dunlop et al., 2012). For example, in depression, non-responders are either given a different SSRI, non-SSRI antidepressant or CBT, with little data to support therapeutic selection (Dunlop et al., 2012) and as yet, no predictors of treatment outcome in anxiety disorders have been established (Deckert and Erhardt, 2019). Therefore, biomarker discovery to guide selection of treatment type is an important task in the field of psychiatric research.

Candidate biomarkers, such as brain structures within the frontal and temporal lobes have been implicated in emotion processing (Ochsner & Gross, 2008), and studies suggest the involvement of these regions in the pathology of IPs such as MDD (Joormann & Stanton, 2016; Singh et al., 2013) and GAD (Greening & Mitchell, 2015; Mennin et al., 2002; Sheline, 2003). For example, one group that applied graph analysis to examine gray matter networks (Singh et al., 2013) found higher right amygdala network centrality and found that there were fewer significant frontal lobe network hubs in MDD compared to healthy controls. In a diffusion-tensor imaging study comparing GAD and healthy control structural connectivity, connections between the amygdala and anterior cingulate cortex were found to be stronger in GAD, whereas connections between the amygdala frontal lobe regions, such as the medial orbital cortex, were weaker compared to healthy controls (Greening & Mitchell, 2015).

These brain regions do not function or exist in isolation, and as such it is important to consider the interconnections that they have with the rest of the brain. Many of these regions are connected to one another by the uncinate fasciculus (UF), a white matter tract that links the orbitofrontal cortex with temporal regions including the amygdala and hippocampus (Catani et al., 2002; Schmahmann et al., 2007). Many studies have found significant associations between the UF and IPs. Fractional anisotropy (FA), a measure of white matter

integrity, has been found to be decreased in the left and right UF in MDD (Harada et al., 2016; Zhang et al., 2012; Zheng et al., 2018), social anxiety disorder (SAD) (Phan et al., 2009) and generalized anxiety disorder (GAD) (Ayling et al., 2012).

One method of studying the structure or function of the brain is to model it as a network and investigate the graph theory measures of the network (Bullmore & Sporns, 2009). A graph is composed of nodes, e.g., brain regions, and edges, e.g., a “distance” measure between each region. These graphs have quantifiable features that describe specific network properties. Common metrics include strength, clustering coefficient, efficiency and centrality (see Methods for details). In this study, we use diffusion tensor imaging to generate structural connectomes for each individual. Graph edge weights are determined by the number of fibers within the white matter tract connecting each node. We examine the global properties of each subject’s network and focus on the subnetwork of nodes connected by the UF when examining local network properties.

Canonically, depression, anxiety and other IPs have been classified as separate disease entities, and have thus been studied and treated as such. Each pathology is characterized by an aspect of mood dysregulation: for example, rumination (persistent negative thoughts about the past) is most typical of depression, whereas worry (persistent negative thoughts about the future) is more representative of anxiety (Spasojevic & Alloy, 2001; Borkovec et al., 2004). Because both of these disorders are responsive to the same types of therapy and both share a comparably dysfunctional cognitive positive feedback process, it may be that they share a similar neuropathological substrate. In addition, as discussed above, there is evidence to suggest the presence of such a common neural disease process that would distinguish IP patients and healthy individuals. While the integrity of the UF itself has been previously assessed and pathologically implicated in the context of several IPs, it has not yet been evaluated in a transdiagnostic sample. We also, for the first time, conduct an exploratory analysis of the graph measures of the structural connectomes of such a sample, with a focus on the features of the brain regions within the UF subnetwork, including the amygdala, hippocampus and orbitofrontal lobe gyri.

The goal of the present study is three-fold: 1) to investigate whether there are baseline differences in white matter network properties and integrity between HC and PT to identify unifying features that may be common to all IPs, 2) to determine whether these properties change with treatment and if these changes are treatment modality specific and 3) to determine if network properties predict treatment response across modalities or in a modality specific way. First, we determined whether UF white matter integrity is abnormal in our cohort of IP patients (PT) compared to healthy controls (HC) by measuring the fractional anisotropy (FA) of the UF. We then characterize baseline differences in network properties between HC and PT to identify unifying features that may be common to all IPs. It was also examined whether any baseline network measures predicted treatment response to either treatment modality by correlating baseline graph metrics with improvement in clinical assessment scores. Next, we examined the effect of treatment with either CBT or SSRI on these network measures. To assess whether changing measures may represent neural substrates of treatment response, the correlation between change in metric and treatment response is assessed. Additionally, we evaluate the stability of networks in the HC

group over time. While this is a preliminary pilot study to examine the UF subnetwork, we anticipated that we would find reduced bilateral UF white matter integrity. In addition, we expect that graph theory metrics will indicate stronger network influence of limbic areas and decreased influence of frontal regions in PT vs HC. Furthermore, we predict that these network properties may either change with 12 weeks of SSRI or CBT treatment or predict treatment response, aiding in the selection of treatment modality for a large transdiagnostic sample of the psychiatric population.

2. Methods

2.1. Subjects and clinical trial

Subjects were recruited from the greater Chicago area through advertisements and through University of Illinois at Chicago (UIC) outpatient clinics and counseling centers as part of a larger Research Domain Criteria (RDoC) (Cuthbert, 2014) investigation on predictors of IP treatment outcomes ([ClinicalTrials.gov](https://clinicaltrials.gov/ct2/show/study/NCT01903447) identifier: [NCT01903447](https://clinicaltrials.gov/ct2/show/study/NCT01903447)). A heterogeneous study population was recruited in order to obtain a sample with a broad range of symptom severity and functioning. A total of 69 subjects with an IP and 24 healthy controls were assessed at baseline. 24 IP subjects completed the study (11 in the SSRI cohort, 13 in the CBT cohort), and were used for Pre vs. Post analyses. Details regarding inclusion/exclusion criteria, participant recruitment, clinical characteristics and treatment have been previously described (Gorka et al., 2019). In brief, this study was approved by the UIC Institutional Review Board, and written informed consent was obtained for each participant. The inclusion criteria for subjects were age between 18 and 65 years, and the need for randomization to 12 weeks of treatment with SSRI or CBT, as determined by a consensus panel consisting of at least three trained clinicians or study staff. Subjects were excluded from the study if they have a history of current or past manic/hypomanic episodes or psychotic symptoms, active suicidal ideation, presence of contraindications or history of SSRI resistance (no response to >2 SSRIs despite adequate duration and dose), psychopathology not appropriate for the treatment algorithm, or current cognitive dysfunction or impairment. The SCID-5 (First et al., 2015) was used to determine current and lifetime Axis I diagnoses.

The study was a parallel group randomized control trial with 1:1 allocation ratio to either 12 weeks of CBT or SSRI. For the SSRI cohort, PTs were administered one of 5 drugs (sertraline, fluoxetine, paroxetine, escitalopram or citalopram) with a flexible dosing schedule with a goal of obtaining target dose by 8 weeks. SSRI PTs met at 0, 2, 4, 8 and 12 weeks with their study psychiatrist for medication management. For the CBT cohort, PTs received 12 once-weekly 60 minute sessions led by a PhD-level clinical psychologist. CBT procedures were based on the PT's principal diagnosis and predominant symptoms (Burkhouse, 2019). At the time of enrollment (Pre) and after 12 weeks of treatment (Post), severity of IP was assessed with the clinician-administered Hamilton Anxiety Rating Scale (HAMA)(Hamilton, 1959) and the Hamilton Depression Rating Scale (HAMD)(Hamilton, 1986), and self-reported the Depression, Anxiety and Stress Scale (DASS)(Brown et al., 1997), and MRI scans were administered.

2.2. MRI data acquisition and processing.

A diffusion tensor imaging (DTI) scheme was used, and a total of 32 diffusion sampling directions with 4 b0 images were acquired on a 3 Tesla GE Discovery MR750 System (Milwaukee, WI) at the UIC Center for Magnetic Resonance Research. The b-value was 1000 s/mm². The in-plane resolution was 0.9375 mm. The slice thickness was 2.5 mm. Two sets of DTI images were acquired, with opposite phase encoding directions. Each participant was scanned at enrollment (Pre) and at 12 weeks after the initial scan (Post). IP subject Pre scans were acquired before treatment was administered, and Post scans were acquired following 12 weeks of treatment. Healthy controls did not receive treatment but completed the same tasks at the same time points as patients. For preprocessing, the two sets of DTI images were realigned and corrected for motion artifacts and eddy current induced distortions using the FMRIB Software Library (FSL) (Jenkinson et al., 2012). White matter tract reconstruction and fractional anisotropy quantification was done using DSI Studio software (Yeh, et al., 2013). A deterministic fiber tracking algorithm was used. The Automated Anatomical Labeling (AAL) atlas was used for brain parcellation (Tzourio-Mazoyer et al., 2002) into regions of interest (ROIs).

2.3. Graph theoretical analysis.

DSI Studio software was also used to generate an adjacency matrix corresponding to each participant's white matter structural connectome, and to calculate graph theory metrics for each subject. Edge weights correspond to the number of reconstructed fibers passing between each ROI. From the adjacency matrix, graph measures were calculated that represent the network organization of each connectome. In this case, a higher edge weight corresponds to a stronger connection between each node. Path length between two nodes, therefore, is the inverse of the edge weight connecting them.

On the whole brain level, three metrics were calculated for each participant's connectome: global efficiency, density and average clustering coefficient. Efficiency between two nodes is defined as the inverse of the shortest path between them, whereas global efficiency is the average of all node by node efficiencies (Ek, et al., 2015). Network density is defined as the total number of binary node by node connections divided by the total number of all possible connections. Clustering coefficient is defined as the number of connections that exist between the nearest neighbors of a node divided by the number of all possible connections. This can be extended to a global level by computing the average of all nodal clustering coefficients.

At the nodal level, four metrics were computed: nodal strength, local efficiency (LE), clustering coefficient (CC) and betweenness centrality (BC). Nodal strength is defined as the sum of all edges that connect to a node. LE is global efficiency of the subgraph of nodes that are immediate neighbors to the node of interest. Local CC is defined as described above. Finally, BC of a node is the number of shortest paths in the network that pass through the node (Bullmore & Sporns, 2009). Local metrics were calculated using the whole connectome, but downstream nodal analysis was restricted to the uncinate fasciculus subnetwork, which includes (bilateral); the amygdala, hippocampus and inferior, middle, medial and superior frontal orbital cortices (as parcellated by the AAL atlas).

2.4. Statistical analysis.

2.4.1. Between and within group comparisons.—Comparisons of demographics were done using either two-tailed t-tests (i.e., independent or paired t-tests) or Chi-square tests. Comparisons of clinical assessment scores and fractional anisotropy (FA) were performed using two tailed t-tests. Baseline correlation of graph measures and FA vs. clinical score were performed using Spearman correlations. For between group (e.g., baseline) and within group (e.g., Pre vs Post) comparisons, nonparametric permutation tests (10,000 permutations) were used in place of parametric tests (e.g., ANCOVA, Student's t-tests) due to non-normality of graph parameters. Uncorrected p -values are the proportion of times that the null distribution mean difference was greater in magnitude than the mean difference between each group being compared. The level of education (in years) differed significantly between healthy controls and patients at baseline and was treated as a nuisance variable by regressing out level of education effects and performing permutation analyses on the residuals. This is reported as the adjusted p -value. To correct for multiple comparisons, false discovery rate (FDR) control was employed with $n=12$ (number of nodes within the UF subnetwork) (Benjamini & Hochberg, 1995). This was done on uncorrected p -values and adjusted p -values, reported as q -values and adjusted q -values, respectively. The mean effect, determined as the percentage difference of group means, was calculated by (PT-HC)/HC or (Post-Pre)/Pre for baseline and Pre vs. Post comparisons, respectively. Cohen's d was reported as effect size and was calculated by (PT-HC)/sd(pooled), where sd(pooled) is the pooled standard deviation of all subjects.

2.4.2. Prediction of treatment response.—To determine whether graph theory metrics are predictive of treatment response, baseline graph metric values were correlated (using Spearman correlations due to non-normality) with Pre minus Post clinical assessment scores (positive numbers represent clinical improvement). FDR was used on the correlation p -values with $n=12$, and only correlations with $q<0.2$ were reported.

2.4.3. Correlates of treatment response.—For any measure that was shown to significantly change with treatment ($p<0.05$, Pre vs. Post), Spearman correlations were performed between the change in metric (Post-Pre, where positive differences indicate metric growth following treatment) change in clinical assessment score (Pre-Post, indicating clinical improvement). FDR correction was done with $n=7$ (the total number of correlations performed). Only correlations with $p<0.05$ are reported.

3. Results

3.1. Demographic and clinical information

Table and figure 1 summarize the demographic and clinical information of patients (PT) and healthy controls (HC). To control effects of confounding variables, e.g., the wide age range of our sample, we performed t-tests on demographic variables between all PT and HC, as well as between SSRI and CBT cohorts. There was a significant difference in the amount of years of education between HC and PT ($p=0.008$). Therefore, education was treated as a nuisance variable by regressing out level of education effects and performing permutation analyses on the residuals. No other differences were found between all PT and HC. In

addition, there were no significant baseline differences in demographics or clinical assessment scores between the SSRI and CBT cohorts. Of note, although there is a large age range in our sample, there was found to be no significant difference in age between the cohorts. In addition, age did not correlate with any of the graph theory metrics in our sample at baseline. All clinical scores were found to significantly decrease following treatment in each cohort. Additionally, comorbidity is intentionally common in our patient sample, and it is skewed towards anxiety diagnoses. In all PT, 53% have a mood disorder, and 90% have an anxiety disorder. Similarly, in SSRI and CBT, anxiety and mood disorders are present in 36% and 91%, and 38% and 100%, respectively.

3.2. White matter integrity of the uncinate fasciculus

To assess white matter integrity, we determined fractional anisotropy (FA) for the left and right uncinate fasciculus (UF). A significant reduction in left UF FA was present pre-treatment in PT relative to HC (fig 2D). This reduction was no longer present post-treatment, or in the right UF at either time point. Additionally, within the HC group there was no change in UF FA. Baseline measures of FA did not correlate significantly with baseline clinical assessment scores within PT group.

3.2. Baseline differences and correlation with symptom severity in graph theory measures.

At the global level, we found no significant differences in graph measures between PT and healthy controls HC at baseline. However, we did find significant differences in local measures between PT and HC (table 2). Of these results, only three remained significant when treating years of education as a nuisance factor in the permutation test (*adj-p*); left frontal mid orbital clustering coefficient (CC) ($p=0.014$, $adj-p=0.027$, *mean effect*: +32.7% in PT), left frontal mid orbital betweenness centrality (BC) ($p=0.017$, $adj-p=0.022$, *mean effect*: -28.7% in PT) and right amygdala BC ($p=0.013$, $adj-p=0.034$, *mean effect*: +50.4% in PT). No differences survived FDR, but right amygdala and left frontal mid orbital BC were at threshold (both $q=0.200$). We found no significant correlations between baseline clinical assessment scores and any graph theory measure after false discovery rate control ($n=12$ =number of ROIs).

3.3. Treatment effect on graph theory measures

Similar to above, analysis of global graph measures revealed no treatment or time dependent significant differences in either patient cohort or in healthy controls. Significant nodal graph measure differences were found only when patients were segregated by treatment (table 3). In the SSRI cohort, the only significantly different Pre vs Post metrics were BC of the left frontal superior ($p=0.044$, $q=0.262$, +78.7% post-treatment) and inferior ($p=0.016$, $q=0.197$, -45.5% post-treatment) orbital cortices. In the CBT cohort only one finding survived FDR correction and had an adequate effect size: left frontal medial orbital local efficiency (LE) ($p=0.03$, $q=0.167$, +20.6% post-treatment). No local metric changes were appreciated in HC between timepoints.

3.4. Graph theory measures as predictors of treatment response

To determine whether graph measures in patients could predict treatment response, we correlated all baseline measures with improvement in clinical assessment scores (table 4). In order to reduce false positive correlations, we performed false discovery rate correction on the results of the correlations with $n=12$ ROIs. Similar to above findings, no global measures predicted treatment response. Local metrics were found to correlate significantly only when patients were segregated by treatment modality. In the SSRI cohort, the right frontal superior orbital cortex BC was found to correlate with HAMA improvement ($p=0.011$, $q=0.128$, $\rho=0.731$). Most of the significant correlations that survived FDR correction ($q<0.2$) were found in the CBT cohort. Left frontal medial orbital cortex ($p=0.039$, $q=0.158$, $\rho=-0.576$) and left and right hippocampus ($p=0.005$, $q=0.055$, $\rho=-0.730$; $p=0.037$, $q=0.158$, $\rho=-0.581$, respectively) LE negatively correlated with DASS improvement, while right frontal inferior orbital strength correlated negatively with HAMD improvement ($p=0.006$, $q=0.071$, $\rho=-0.716$).

3.5. Graph measures as correlates of treatment response

To investigate the relationship between graph measures and treatment response, we correlated mean differences between graph measures that significantly changed with treatment and improvement in clinical assessment scores (HAMD, HAMA and DASS). The only significant correlations were found in the CBT cohort (table 5). Post-Pre changes in left frontal medial orbital CC ($p=0.042$, $q=0.084$, $\rho=0.57$) and LE ($p=0.019$, $q=0.075$, $\rho=0.639$), as well as left frontal superior orbital CC ($p=0.008$, $q=0.064$, $\rho=0.694$) positively correlate with DASS improvement.

4. Discussion

4.1. White matter integrity of the uncinate fasciculus

Similar to previous findings, we found a significant decrease in left uncinate fasciculus (UF) fractional anisotropy (FA) in PT versus HC at baseline. Laterality of UF findings, does differ between studies, however, with decreased FA found in left only (Murphy et al., 2012), right only (Zhang et al., 2012), or bilateral (Zheng et al., 2018) UF. In SAD and GAD, decreased FA was also found in the right UF of PTs (Phan et al., 2009, Ayling et al., 2012). We did not find an effect of treatment on UF FA. This is true whether patients are aggregated or split by cohort (data not shown). Fewer studies have examined if treatment alters the FA of the UF. In experiments with SSRI as treatment, either left (Zheng et al., 2018) or right (Lai et al., 2013) UF FA was found to increase with treatment. It should be noted that the role of the UF in other disorders of emotion regulation is less clear. Findings in bipolar disorder are mixed, with either decreased or equal levels of UF FA found in PTs. In a study looking at patients with panic disorder there was no change in FA compared to HCs (Jenkins et al., 2016). Nonetheless, our findings suggest the importance of the role of UF white matter integrity in the pathology of internalizing psychopathologies (IPs).

4.2. Baseline differences in graph measures

On the whole brain level, there were no significant differences in graph measures between PT ($n=69$) and HC ($n=24$). This is in line with previous studies of MDD brain networks that have generally found limited (Ajilore et al., 2014; Qin et al., 2014) or no significant differences (Korgaonkar et al., 2014; Lim et al., 2013) in global metrics of clustering coefficient, strength and characteristic path length. At the local (i.e., nodal) level, we found several significant differences ($p<0.05$, uncorrected) in metrics between HC and PT (table 2). Of these results, only three remained significant when treating years of education as a nuisance factor in the permutation test (*adj-p*); left frontal mid orbital clustering coefficient (CC), left frontal mid orbital betweenness centrality (BC) and right amygdala BC. No differences survived FDR, but right amygdala and left frontal mid orbital BC were at threshold (both $q=0.200$).

When considering these two most statistically significant results, a trend of increased subcortical-limbic (amygdala) centrality and decreased cortical centrality in PT compared to HC emerges. BC is a measure of nodal importance in the network, proportional to the amount of shortest paths that pass through said node. Thus, our results indicate that the right amygdala may be a more influential node in the brain networks of IP PTs, while the left frontal mid orbital cortex is less influential, compared to HCs. This is consistent with a prevailing theory of emotion dysregulation in the internalizing pathologies: impaired “top-down” influence of prefrontal regions on limbic structures, via subcortical disinhibition or overactivity. Often, this is shown by increased amygdala activity or influence in the context of IPs. In MDD, amygdala BC and degree was found to be increased in grey matter volume (Singh et al., 2013) and fMRI networks (Gong & He, 2015; Jin et al., 2011), respectively. In studies of anxiety disorders, amygdala volume correlated with trait anxiety and amygdala activity was found to be increased as measured by positron emission tomography (PET) and fMRI in GAD, SAD and PTSD. There is also ample evidence of frontal cortical disturbances in the IPs. In a negative thought suppression task, left frontal mid orbital cortex activity was decreased in MDD compared to HCs, demonstrating a potential neural substrate for decreased emotion regulation (Carew et al., 2013). In another MDD study, left frontal superior and middle orbital gyrus centralities were decreased in PT vs HC (Zhang et al., 2011). Frontal lobe regions in general were found to be less influential in the fMRI networks of individuals with MDD compared to HCs via a network based statistic analysis (Korgaonkar et al., 2014). Similar results have been obtained in studies of anxiety. Greening and colleagues found that trait anxiety can be predicted by decreased connectivity between the amygdala and frontal lobes (Greening & Mitchell, 2015). Finally, individuals with PTSD were found to have hypoactivity of the ventromedial prefrontal cortex compared with healthy controls (Etkin & Wager, 2007). The sum of these findings are validated by our own, indicating that all IPs may share common dysfunction of the limbic frontal interactions.

4.3. Graph theory metric predictors of treatment response

Next, we sought to determine whether any graph theory metrics may serve as predictors of treatment response in general, or if there are unique predictors for each type of treatment examined (SSRI or CBT). Consistent with above findings, we did not identify any significant correlations between global graph metrics and treatment response with cohorts

aggregated or segregated. At the local level, we only found significant correlations when patients were segregated by treatment modality.

In the SSRI cohort, the right frontal superior orbital cortex BC was found to negatively correlate with HAMA improvement. This correlation, however, is in the opposite direction of nodal strength with both cohorts aggregated, as higher levels of baseline measures of BC in this region are predictive of better response to treatment. This suggests that nuanced network architecture of frontal cortical networks plays an important role in treatment response, such that right superior orbitofrontal network influence (measured by BC) is beneficial, whereas overall strength of connectivity, may be undesired without more specific network organization. Our preliminary findings indicate that individuals with greater right superior orbitofrontal BC may be good candidates for SSRI based therapy.

As before, the CBT cohort analysis yielded the greatest number of significant results. Several correlations were present between score improvement and graph metrics for subcortical nodes: baseline LE of the bilateral hippocampi negatively correlate with clinical improvement. This suggests that those individuals with brain networks that allow for more efficient information transduction to and from these limbic nodes are less responsive to treatment with CBT. Of interest, the left frontal medial orbital cortex LE also negatively correlated with DASS improvement (see table 3). As mentioned above, we found a positive correlation between change (Post-Pre) in this metric and clinical improvement, indicating that greater increases in this metric are associated with greater response to CBT. These results suggest that the left medial orbitofrontal LE is a brain network substrate for CBT, and that if individuals have a higher baseline value in this region, that they may not be able to further benefit from the neural changes associated with CBT. Previous studies have identified similar correlations between left prefrontal cortical regional volumes (Seminowicz et al., 2013) and fMRI activities during self-referential processing of negative stimuli (Yoshimura et al., 2014) and CBT response, but this is the first report, to our knowledge, of left medial orbitofrontal changes in response to CBT when examined with graph theory metrics of the structural connectome.

4.4. Changes in graph measures with treatment and correlates of treatment response

(Pre) versus after (Post) treatment in either aggregated PTs, or PTs split by cohort (SSRI or CBT). Interestingly, significant differences on the nodal level were only appreciable when PTs were split by cohort, suggesting the possibility of treatment specific effects on white matter networks in IP PTs. Of note, there were no significant differences found in any metrics, global or local, at baseline, between PT cohorts (SSRI or CBT). Neither were there any differences in HCs between timepoints suggesting stability in network properties in HCs over time. Additionally, we found no significant correlations between baseline metrics and baseline symptom severity in either grouped or segregated cohorts (data not shown). Furthermore, our most significant results are almost all found in frontal cortical metrics, with only one subcortical region being identified, and only in the CBT cohort.

In the SSRI cohort, the only significantly different Pre vs Post metrics were an increased BC of the left frontal superior and decrease in BC of the inferior orbital cortices. Results of previous studies of the effects of SSRIs in MDD are somewhat mixed, but generally report

increased activity or connectivity of orbitofrontal regions following treatment (Goldapple et al., 2004; Posner et al., 2013; Wang et al., 2015), while others report an opposite effect (Li et al., 2013). In a study comparing treatment resistant and treatment refractory MDD, the left orbitofrontal inferior and superior cortices were found to be increased and decreased, respectively, in treatment refractory MDD only (Hou et al., 2016). Our findings suggest that the left orbitofrontal inferior and superior cortex BC decrease and increase, respectively with treatment. It could be that SSRI treatment helps to normalize the network role of these brain regions towards HC, but we did not find a significant difference at baseline. Our results support the general notion that SSRIs may have an effect on the frontal cortical brain networks of individuals with IPs, but our modest sample size ($n=11$) limits the interpretation of our findings. Our most significant treatment effects were found in the CBT cohort, but only one finding survived FDR correction and had an adequate effect size: left frontal medial orbital LE (increase following treatment). LE measures the capacity of a node to transmit information to other nodes in the network (Latora & Marchiori, 2001). Our findings suggest that CBT may increase the ability of frontal control networks to propagate information to other nodes in the brain networks of individuals with IPs.

We next determined if any of the graph measures that were found to change with treatment ($p<0.05$, uncorrected) correlated with measures of treatment response, resulting in significant correlations only within the CBT cohort. All three findings were positive correlations of Post-Pre metric vs DASS improvement (meaning that the greater the increase in metric, the greater the symptomatic improvement) of left frontal superior orbital CC and left frontal medial orbital CC and LE (table 5). These results suggest that response to CBT is associated with the gain of cortical efficiency in IPs. Indeed, these findings supports the notion that loss of cortical dominance over limbic structures may be a pathophysiologic substrate of loss of emotion regulation in IPs, that CBT may help to reverse this dysregulation, and that treatment response to CBT may be dependent on the gain of cortical efficiency. It has been found previously that CBT results in increased orbitofrontal cortical activation, measured via fMRI, during an emotion regulation task in post versus pre treatment MDD PTs, further suggesting the ability of CBT to ameliorate the loss of cortical control of emotion(Ritchey et al., 2011).

4.5. Limitations

There are general limitations that must be considered with the present study. While the sample size of our baseline analysis is moderate (PT $n=69$, HC $n=24$), the number of participants that completed study is less than half of the starting population (HC $n=10$, SSRI $n=11$, CBT $n=13$). Given the sample size, our findings must be considered as preliminary and need be replicated in a larger transdiagnostic cohort of patients with internalizing psychopathologies. Finally, our sample is skewed towards PTs with anxiety disorders over mood disorders: almost all patients have anxiety disorders, whereas mood disorders are present in 53% of all PTs, and 36–38% of PTs in the SSRI and CBT cohorts. This is not problematic *per se*, but may limit the generalizability of our findings to the understanding of patients with an isolated mood disorder, such as MDD.

4.6. Conclusion

This study showed that there are baseline differences of nodal graph measures in an IP cohort compared to HCs, suggesting that there are common neuropathologic substrates shared trans-diagnostically. Our results suggest that there is baseline higher cortical and lower amygdala network influence, which is in agreement with previous findings in the literature. Changes in graph theoretical metrics following treatment mostly involves cortical regions and appears to be modality specific, suggesting that CBT and SSRI treatment uniquely effect white matter brain networks. In addition, we show that there are nodal predictors of general and modality specific treatment response, that suggest that greater baseline limbic network influence results in lesser response to therapy. Overall, this study provides insight to shared white matter network features that may be aberrant across the swath of internalizing psychopathologies, and shed light on potential biomarkers to help guide treatment selection for these common disorders.

Acknowledgements.

We would like to thank Fang-Cheng Yeh (University of Pittsburg) for his assistance in implementing DSI Studio software for data processing and figure generation. This study was funded by the National Institute of Mental Health of the National Institutes of Health (NIMH-NIH) grant R01MH101497 (to KLP). PJT is funded by the NIH-NIMH grant 5T32MH067631-14 to Mark Rasenick, Department of Physiology and Biophysics, University of Illinois at Chicago, Chicago, IL, USA. All authors declare no conflicts of interest.

References.

- Ajilore O, Lamar M, Kumar A, 2014 Association of brain network efficiency with aging, depression, and cognition. *Am. J. Geriatr. Psychiatry* 22, 102–110. 10.1016/j.jagp.2013.10.004 [PubMed: 24200596]
- Ayling E, Aghajani M, Fouche JP, van der Wee N, 2012 Diffusion tensor imaging in anxiety disorders. *Curr. Psychiatry Rep* 14, 197–202. 10.1007/s11920-012-0273-z [PubMed: 22460663]
- Benjamini Y, Hochberg Y, 1995 Controlling the False Discovery Rate: A Practical and Powerful Approach to Multiple Testing. *J. R. Stat. Soc. Series B. Stat. Methodol* 57, 289–300. 10.1111/j.2517-6161.1995.tb02031.x
- Brown TA, Chorpita BF, Korotitsch W, Barlow DH, 1997 Psychometric properties of the Depression Anxiety Stress Scales (DASS) in clinical samples. *Behav. Res. Ther* 35, 79–89. 10.1016/S0005-7967(96)00068-X [PubMed: 9009048]
- Bullmore E, Sporns O, 2009 Complex brain networks: graph theoretical analysis of structural and functional systems. *Nat. Rev. Neurosci* 10, 186–198. 10.1038/nrn2575 [PubMed: 19190637]
- Burkhouse KL, Jimmy J, Defelice N, Klumpp H, Ajilore O, Hosseini B, Fitzgerald KD, Monk CS and Phan KL, 2019 Nucleus accumbens volume as a predictor of anxiety symptom improvement following CBT and SSRI treatment in two independent samples. *Neuropsychopharmacology*. 45, 1–9. 10.1038/s41386-019-0575-5 [PubMed: 31486776]
- Borkovec TD, Alcaine O, Behar E, 2004 Avoidance theory of worry and generalized anxiety disorder. *Generalized anxiety disorder: Advances in research and practice*. Guilford Press, New York.
- Carew CL, Milne AM, Tatham EL, MacQueen GM, Hall GBC, 2013 Neural systems underlying thought suppression in young women with, and at-risk, for depression. *Behav. Brain Res* 257, 13–24. 10.1016/j.bbr.2013.09.016 [PubMed: 24055881]
- Catani M, Howard RJ, Pajevic S, Jones DK, 2002 Virtual in Vivo Interactive Dissection of White Matter Fasciculi in the Human Brain. *NeuroImage*. 17, 77–94. 10.1006/nimg.2002.1136 [PubMed: 12482069]
- Cuthbert BN, 2014 The RDoC framework: facilitating transition from ICD/DSM to dimensional approaches that integrate neuroscience and psychopathology. *World Psychiatry*. 13, 28–35. [PubMed: 24497240]

- Deckert J, Erhardt A, 2019 Predicting treatment outcome for anxiety disorders with or without comorbid depression using clinical, imaging and (epi) genetic data. *Curr. Opin. Psychiatry* 32, 1–6. 10.1097/YCO.0000000000000468 [PubMed: 30480619]
- Dunlop BW, Binder EB, Cubells JF, Goodman MM, Kelley ME, Kinkead B, Kutner M, Nemeroff CB, Newport DJ, Owens MJ and Pace TW, 2012 Predictors of remission in depression to individual and combined treatments (PRE-DICT): study protocol for a randomized controlled trial. *Trials*. 13, 106 10.1186/1745-6215-13-106 [PubMed: 22776534]
- Ek B, VerSchneider C, Narayan DA, 2015 Global efficiency of graphs. *AKCE Int. J. of Graphs Comb* 12, 1–13. 10.1016/j.akcej.2015.06.001
- Etkin A, Wager TD, 2007 Functional Neuroimaging of Anxiety: A Meta-Analysis of Emotional Processing in PTSD, Social Anxiety Disorder, and Specific Phobia. *Am. J. Psychiatry* 164, 1476–1488. 10.1176/appi.ajp.2007.07030504 [PubMed: 17898336]
- First MB, Williams JBW, Karg RS, Spitzer RL., 2015 Structured Clinical Interview for DSM-5-Research Version (SCID-5 for DSM-5, Research Version; SCID-5-RV). American Psychiatric Association, Arlington, VA.
- Goldapple K, Segal Z, Garson C, Lau M, Bieling P, Kennedy S, Mayberg H, 2004 Modulation of cortical-limbic pathways in major depression: treatment-specific effects of cognitive behavior therapy. *Arch. Gen. Psychiatry* 61, 34–41. 10.1001/archpsyc.61.1.34 [PubMed: 14706942]
- Gong Q, He Y, 2015 Depression, Neuroimaging and Connectomics: A Selective Overview. *Biol. Psychiatry* 77, 223–235. 10.1016/j.biopsych.2014.08.009 [PubMed: 25444171]
- Gorka SM, Young CB, Klumpp H, Kennedy AE, Francis J, Ajilore O, Langenecker SA, Shankman SA, Craske MG, Stein MB, Phan KL, 2019 Emotion-based brain mechanisms predictors for SSRI and CBT treatment of anxiety and depression: a randomized trial. *Neuropsychopharmacology*. 44,1639–1648. 10.1038/s41386-019-0407-7 [PubMed: 31060042]
- Greening SG, Mitchell DGV, 2015 A network of amygdala connections predict individual differences in trait anxiety. *Hum. Brain Mapp* 36, 4819–4830. 10.1002/hbm.22952 [PubMed: 26769550]
- Hamilton M, 1959 The assessment of anxiety states by rating. *Br. J. Med. Psychol* 32, 50–55. 10.1111/j.2044-8341.1959.tb00467.x [PubMed: 13638508]
- Hamilton M, 1986 The Hamilton Rating Scale for Depression. *Assessment of Depression*. 143–152. Springer, Berlin, Heidelberg 10.1007/978-3-642-70486-4_14
- Harada K, Matsuo K, Nakashima M, Hobara T, Higuchi N, Higuchi F, Nakano M, Otsuki K, Shibata T, Watanuki T, Matsubara T, 2016 Disrupted orbitomedial prefrontal limbic network in individuals with later-life depression. *J. Affect. Disord* 204, 112–119. 10.1016/j.jad.2016.06.031 [PubMed: 27344619]
- Hou Z, Wang Z, Jiang W, Yin Y, Yue Y, Zhang Y, Song X, Yuan Y, 2016 Divergent topological architecture of the default mode network as a pretreatment predictor of early antidepressant response in major depressive disorder. *Sci. Rep* 6, 39243 10.1038/srep39243 [PubMed: 27966645]
- Jenkins LM, Barba A, Campbell M, Lamar M, Shankman SA, Leow AD, Ajilore O, Langenecker SA, 2016 Shared white matter alterations across emotional disorders: A voxel-based meta-analysis of fractional anisotropy. *NeuroImage Clin*. 12, 1022–1034. 10.1016/j.nicl.2016.09.001 [PubMed: 27995068]
- Jenkinson M, Beckmann CF, Behrens TEJ, Woolrich MW, Smith SM, 2012 FSL. *NeuroImage*. 62, 782–790. 10.1016/j.neuroimage.2011.09.015 [PubMed: 21979382]
- Jin C, Gao C, Chen C, Ma S, Netra R, Wang Y, Zhang M, Li D., 2011 A preliminary study of the dysregulation of the resting networks in first-episode medication-naïve adolescent depression. *Neurosci. Lett* 503, 105–109. 10.1016/j.neulet.2011.08.017 [PubMed: 21871534]
- Joormann J, Stanton CH, 2016 Examining emotion regulation in depression: A review and future directions. *Behav. Res. Ther* 86, 35–49. 10.1016/j.brat.2016.07.007 [PubMed: 27492851]
- Kessler RC, Chiu WT, Demler O, Walters EE, 2005 Prevalence, Severity, and Comorbidity of 12-Month DSM-IV Disorders in the National Comorbidity Survey Replication. *Arch. Gen. Psychiatry* 62, 617–627. 10.1001/archpsyc.62.6.617 [PubMed: 15939839]
- Klooster DC, Franklin SL, Besseling RM, Jansen JF, Caeyenberghs K, Duprat R, Aldenkamp AP, de Louw AJ, Boon PA, Baeken C, 2019 Focal application of accelerated iTBS results in global

changes in graph measures. *Hum. Brain Mapp* 40, 432–450. 10.1002/hbm.24384 [PubMed: 30273448]

- Korgaonkar MS, Williams LM, Song YJ, Usherwood T, Grieve SM, 2014 Diffusion tensor imaging predictors of treatment outcomes in major depressive disorder. *Br. J. Psychiatry* 205, 321–328. 10.1192/bjp.bp.113.140376 [PubMed: 24970773]
- Kovacs M, Devlin B, 1998 Internalizing disorders in childhood. *J. Child Psychol. Psychiatry* 39, 47–63. 10.1111/1469-7610.00303 [PubMed: 9534086]
- Lai C-H, Wu Y-T, Yu P-L, Yuan W, 2013 Improvements in white matter micro-structural integrity of right uncinate fasciculus and left fronto-occipital fasciculus of remitted first-episode medication-naïve panic disorder patients. *J. Affect. Disord* 150, 330–336. 10.1016/j.jad.2013.04.014 [PubMed: 23680435]
- Latora V, Marchiori M, 2001 Efficient behavior of small-world networks. *Phys. Rev. Lett* 87, 198701 10.1103/PhysRevLett.87.198701 [PubMed: 11690461]
- Li B, Liu L, Friston KJ, Shen H, Wang L, Zeng L-L, Hu D, 2013 A treatment-resistant default mode subnetwork in major depression. *Biol. Psychiatry*, 74, 48–54. 10.1016/j.biopsych.2012.11.007 [PubMed: 23273724]
- Lim HK, Jung WS, Aizenstein HJ, 2013 Aberrant topographical organization in gray matter structural network in late life depression: a graph theoretical analysis. *Int. Psychogeriatr* 25, 1929–1940. 10.1017/S104161021300149X [PubMed: 24093725]
- Mennin DS, Heimberg RG, Turk CL, Fresco DM, 2002 Applying an Emotion Regulation Framework to Integrative Approaches to Generalized Anxiety Disorder. *Clin. Psychol* 9, 85–90. 10.1093/clipsy.9.1.85
- Mothersill O, Donohoe G, 2016 Neural effects of social environmental stress - an activation likelihood estimation meta-analysis. *Psychol. Med* 46, 2015–2023. 10.1017/S0033291716000477 [PubMed: 27216635]
- Murphy ML, Carballedo A, Fagan AJ, Morris D, Fahey C, Meaney J, Frodl T, 2012 Neurotrophic tyrosine kinase polymorphism impacts white matter connections in patients with major depressive disorder. *Biol. Psychiatry* 72, 663–670. 10.1016/j.biopsych.2012.04.015 [PubMed: 22609366]
- Ochsner KN, Gross JJ, 2008 Cognitive Emotion Regulation: Insights From Social Cognitive and Affective Neuroscience. *Curr. Dir. in Psychol. Sci* 17, 153–158. 10.1111/j.1467-8721.2008.00566.x [PubMed: 25425765]
- Phan KL, Orlichenko A, Boyd E, Angstadt M, Coccaro EF, Liberzon I, Arfanakis K, 2009 Preliminary Evidence of White Matter Abnormality in the Uncinate Fasciculus in Generalized Social Anxiety Disorder. *Biol. Psychiatry* 66, 691–694. 10.1016/j.biopsych.2009.02.028 [PubMed: 19362707]
- Posner J, Hellerstein DJ, Gat I, Mechling A, Klahr K, Wang Z, McGrath PJ, Stewart JW Peterson BS, 2013 Antidepressants normalize the default mode network in patients with dysthymia. *JAMA Psychiatry*, 70, 373–382. 10.1001/jamapsychiatry.2013.455 [PubMed: 23389382]
- Qin J, Wei M, Liu H, Yan R, Luo G, Yao Z, Lu Q, 2014 Abnormal brain anatomical topological organization of the cognitive-emotional and the frontoparietal circuitry in major depressive disorder. *Magn. Reson. Med* 72, 1397–1407. 10.1002/mrm.25036 [PubMed: 24273210]
- Ritchey M, Dolcos F, Eddington KM, Strauman TJ, Cabeza R, 2011 Neural correlates of emotional processing in depression: Changes with cognitive behavioral therapy and predictors of treatment response. *J. Psychiatr. Res* 45, 577–587. 10.1016/j.jpsychires.2010.09.007 [PubMed: 20934190]
- Schmahmann JD, Pandya DN, Wang R, Dai G, D'Arceuil HE, de Crespigny AJ, Wedeen VJ, 2007 Association fibre pathways of the brain: parallel observations from diffusion spectrum imaging and autoradiography. *Brain*. 130, 630–653. 10.1093/brain/awl359 [PubMed: 17293361]
- Seminowicz DA, Shpaner M, Keaser ML, Krauthamer GM, Mantegna J, Dumas JA, Newhouse PA, Filippi CG, Keefe FJ, Naylor MR, 2013 Cognitive behavioral therapy increases prefrontal cortex gray matter in patients with chronic pain. *J. Pain* 14 10.1016/j.jpain.2013.07.020
- Sheline YI, 2003 Neuroimaging studies of mood disorder effects on the brain. *Biol. Psychiatry* 54, 338–352. 10.1016/S0006-3223(03)00347-0 [PubMed: 12893109]
- Singh MK, Kesler SR, Hosseini SH, Kelley RG, Amatya D, Hamilton JP, Chen MC, Gotlib IH, 2013 Anomalous Gray Matter Structural Networks in Major Depressive Disorder. *Biol. Psychiatry*, 74, 777–785. 10.1016/j.biopsych.2013.03.005 [PubMed: 23601854]

- Spasojevi J, Alloy LB, 2001 Rumination as a common mechanism relating depressive risk factors to depression. *Emotion*, 1, 25–37. 10.1037/1528-3542.1.1.25 [PubMed: 12894809]
- Tzourio-Mazoyer N, Landeau B, Papathanassiou D, Crivello F, Etard O, Delcroix N, Mazoyer B, Joliot M, 2002 Automated Anatomical Labeling of Activations in SPM Using a Macroscopic Anatomical Parcellation of the MNI MRI Single-Subject Brain. *NeuroImage*. 15, 273–289. 10.1006/nimg.2001.0978 [PubMed: 11771995]
- Wang L, Xia M, Li K, Zeng Y, Su Y, Dai W, Zhang Q, Jin Z, Mitchell PB, Yu X, He Y, 2015 The effects of antidepressant treatment on resting-state functional brain networks in patients with major depressive disorder. *Hum. Brain Mapp* 36, 768–778. 10.1002/hbm.22663 [PubMed: 25332057]
- Yeh F-C, Verstynen TD, Wang Y, Fernández-Miranda JC, Tseng W-YI, 2013 Deterministic Diffusion Fiber Tracking Improved by Quantitative Anisotropy. *PLOS ONE*, 8, e80713 10.1371/journal.pone.0080713 [PubMed: 24348913]
- Yoshimura S, Okamoto Y, Onoda K, Matsunaga M, Okada G, Kunisato Y, Yoshino A, Ueda K, Suzuki SI, Yamawaki S, 2014 Cognitive behavioral therapy for depression changes medial prefrontal and ventral anterior cingulate cortex activity associated with self-referential processing. *Soc. Cogn. Affect. Neurosci*, 9, 487–493. 10.1093/scan/nst009 [PubMed: 23327934]
- Zhang A, Leow A, Ajilore O, Lamar M, Yang S, Joseph J, Medina J, Zhan L, Kumar A, 2012 Quantitative Tract-Specific Measures of Uncinate and Cingulum in Major Depression Using Diffusion Tensor Imaging. *Neuropsychopharmacology*. 37, 959–967. 10.1038/npp.2011.279 [PubMed: 22089322]
- Zhang J, Wang J, Wu Q, Kuang W, Huang X, He Y, Gong Q, 2011 Disrupted brain connectivity networks in drug-naive, first-episode major depressive disorder. *Biol. Psychiatry* 70, 334–342. 10.1016/j.biopsych.2011.05.018 [PubMed: 21791259]
- Zheng KZ, Wang HN, Liu J, Xi YB, Li L, Zhang X, Li JM, Yin H, Tan QR, Lu HB, Li BJ, 2018 Incapacity to control emotion in major depression may arise from disrupted white matter integrity and OFC-amygdala inhibition. *CNS Neurosci. Ther* 24, 1053–1062. 10.1111/cns.12800 [PubMed: 29368421]

HIGHLIGHTS

- Left uncinate fasciculus fiber integrity was decreased in patients vs controls.
- Right amygdala betweenness centrality was higher in patients vs controls.
- Global network measures were not difference in patients vs controls.
- Treatment effects on graph measures were treatment modality specific.
- Graph metric predictors of treatment response were treatment specific.

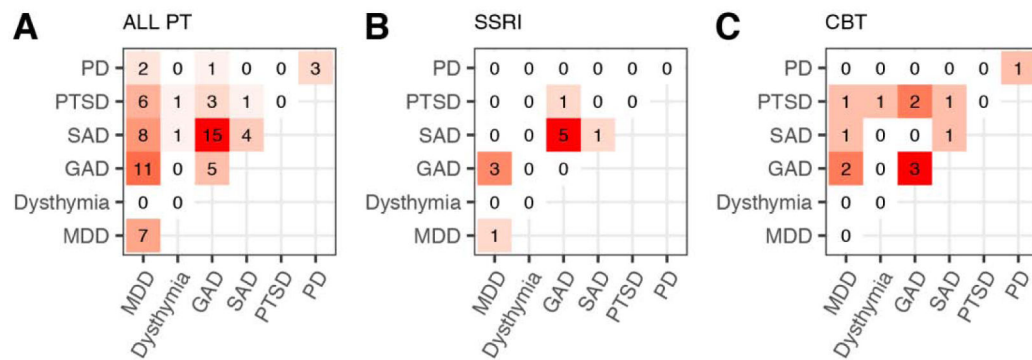


Figure 1. Patient diagnostic information. Each element of the heat map represents the number of patients with comorbidity of diagnoses represented by the corresponding row and column of the element. Elements along the diagonal correspond to patients with only one diagnosis. Heat maps represent all patients at baseline (A), patients in the SSRI cohort (B) and patients in the CBT cohort (C). Abbreviations) PT: patients, SSRI: selective serotonin reuptake inhibitor, CBT: cognitive behavioral therapy, PD: panic disorder, PTSD: post-traumatic stress disorder, SAD: social anxiety disorder, GAD: generalized anxiety disorder, MDD: major depressive disorder.

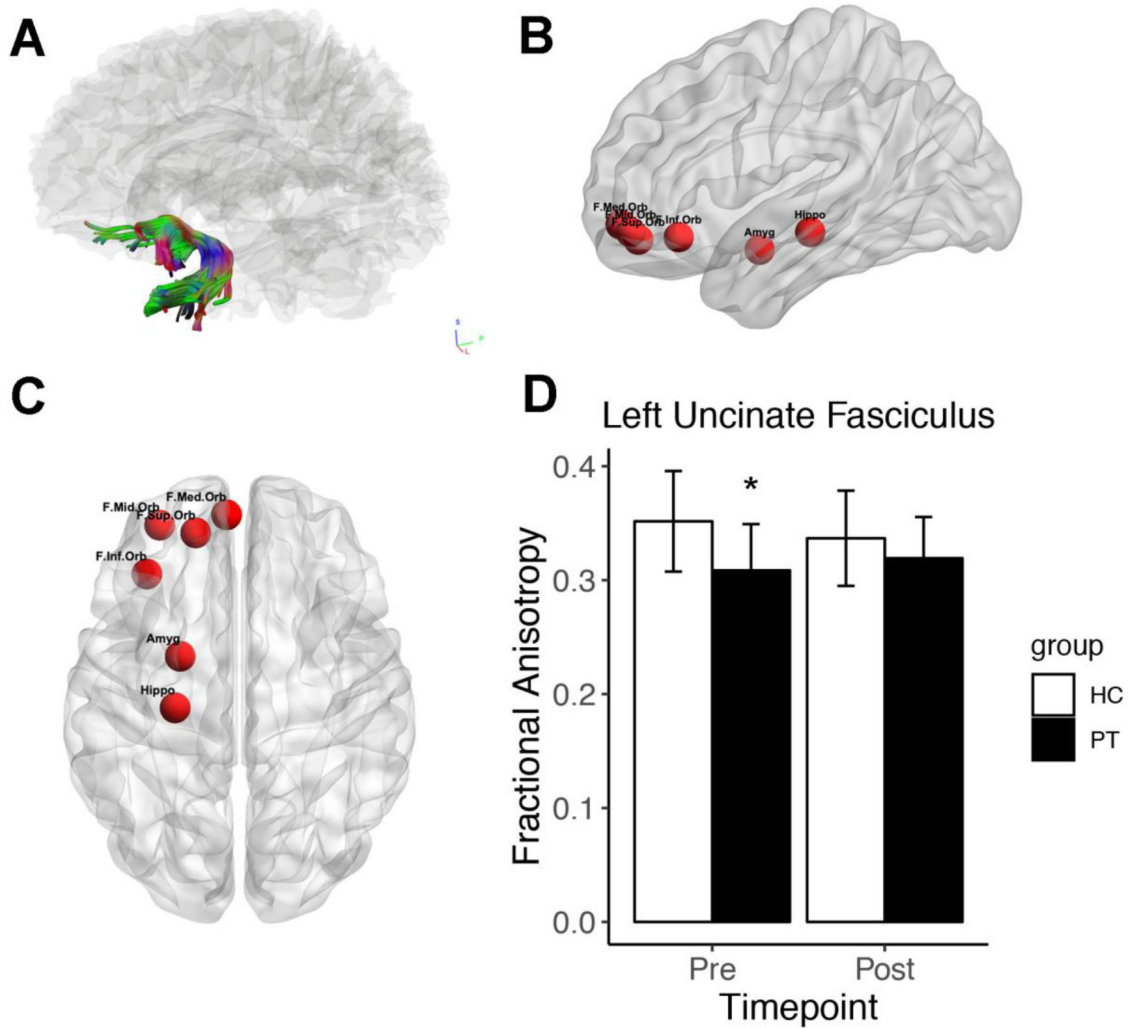


Figure 2.

Overview of the uncinate fasciculus (UF), its subnetwork and fractional anisotropy (FA). A) Reconstruction of representative healthy control UF. B) Sagittal view of left-hand regions of interest (ROIs) in the UF subnetwork. C) Ventral view of left-hand UF subnetwork ROIs. D) FA of the left uncinate fasciculus (UF) in healthy controls (HC) and patients (PT) at baseline (Pre) and 12 weeks later (Post). PTs received 12 weeks of therapy. At baseline, UF FA was significantly decreased in PT relative to HC, determined by two-tailed t-test ($p=0.018$). Abbreviations) F.Med.Orb: frontal medial orbital cortex, F.Mid.Orb: frontal mid orbital cortex, F.Inf.Orb: frontal inferior orbital cortex, F.Sup.Orb: frontal superior orbital cortex, Hippo: hippocampus, Amyg: amygdala.

Table 1.

Participant demographics. A) Demographics of participants used in baseline analysis. Mean years of education was significantly different between groups, determined using a two-tailed t-test ($p=0.008$). B) Demographics and clinical assessment scores of subjects used in Pre vs. Post treatment analysis. All clinical scores significantly decreased following treatment in both treatment cohorts, determined with two-way paired t-tests. Scores did not differ between cohorts at either time point (data not shown). Abbreviations) HC: healthy control, PT: patient, CBT: cognitive behavioral therapy, SSRI: selective serotonin reuptake inhibitor, HAMA: Hamilton anxiety rating scale, HAMD: Hamilton depression rating scale, DASS: depression, anxiety and stress scale.

	Baseline								
	HC (n=24)	All PT (n=69)	Between-group statistics						
	Mean±SD	Mean±SD	t	χ^2	p				
Age (years)	25.2±11.20	28.3±8.4	1.2		0.24				
Gender (M/F)	9/15	22/47		0.063	0.8				
Years of Education	14.6±1.7	16.3±3	3.5		0.0008				
	Pretreatment			Posttreatment		Within-group statistics			
	HC (n=12)	SSRI (n=11)	CBT (n=13)	SSRI (n=11)	CBT (n=13)	SSRI		CBT	
	Mean±SD	Mean±SD	Mean±SD	Mean±SD	Mean±SD	t	p	t	p
Age (years)	25.2±11.2	31.02±12.55	27.17±7.56	31.02±12.55	27.17±7.56				
Gender (M/F)	4/8	3/8	3/10	3/8	3/16				
Years of Education	15.5±1.58	16.54±4.16	16.55±3.56	16.55±3.56	16.54±4.16				
HAMA	NA	19.1±7.62	15.77±6.72	6.2±4.49	6±5.59	4.77	0.00019	4.09	0.00044
HAMD	NA	14.36±4.15	12.23±4.475	5.5±3.37	4.29±3.99	5.39	3.5e-5	4.86	5.9e-5
DASS	NA	31.36±5.5	27.69±6.52	5.9±5.24	6±5.68	10.87	1.4e-9	9.18	2.6e-9
Primary diagnosis	All PT (n=69)	SSRI (n=11)	CBT (n=13)						
GAD	27	5	6						
MDD	17	3	1						
SAD	14	2	3						
PTSD	5	1	1						
PD	5	0	1						
Dysthymia	10	0	1						

Table 2.

Baseline comparison of nodal graph theory metrics in all patients (PT) vs. healthy controls (HC) using permutation tests. Abbreviations) *p*-val: uncorrected permutation test *p*-value, *adj-p*: uncorrected permutation test *p*-value with years of education as a nuisance variable, *q*-val, false discovery rate (FDR) corrected *p*-val, *adj-q*: FDR corrected *adj-p*. For FDR correction, *n*=12 (number of regions of interest). Only nodal metrics that have *p*-val<0.05 are reported. Positive mean effect indicates that mean value of metric is higher in PT than HC. Effect size reported is Cohen's *d*.

cohort	region	metric	p-value	res-p	q-value	res-q	mean effect (%)	effect size
HC vs All PT								
	L Hippocampus	strength	0.046	0.096	0.387	0.576	23.442	-0.470
	L Frontal Mid Orb	clustering coefficient	0.014	0.025	0.168	0.302	32.747	-0.575
	R Frontal Med Orb	clustering coefficient	0.043	0.075	0.237	0.383	23.493	-0.476
	R Frontal Med Orb	local efficiency	0.030	0.067	0.272	0.402	24.426	-0.509
	L Frontal Mid Orb	betweenness centrality	0.018	0.023	0.108	0.203	-28.696	0.548
	R Amygdala	betweenness centrality	0.013	0.034	0.108	0.203	50.394	-0.583

Table 3.

Comparison of baseline (Pre) vs. post treatment (Post), or following 12 weeks in healthy controls (HC), nodal graph theory metrics. Analysis was done with patients (PT) aggregated (All patients) and split by treatment cohort. *P*-values were determined with permutation tests, and are reported uncorrected (*p*-val) and corrected (*q*-val) via false discovery rate (FDR) control with $n=12$ (number of regions of interest). Positive mean effect values indicate that nodal metrics are increased at Post compared to Pre. Effect size is Cohen's *d*. Abbreviations) CBT: cognitive behavioral therapy, SSRI: selective serotonin reuptake inhibitor.

cohort	region	metric	p-value	q-value	mean effect (%)	effect size
All patients					(Pre-Post)/Pre	
	NA	NA	NA	NA	NA	NA
SSRI						
	L Frontal Sup Orb	betweenness centrality	0.043	0.256	78.724	-0.845
	L Frontal Inf Orb	betweenness centrality	0.015	0.176	-45.546	0.970
CBT						
	L Frontal Sup Orb	clustering coefficient	0.037	0.210	33.259	-0.622
	L Frontal Med Orb	clustering coefficient	0.022	0.210	17.730	-0.380
	R Frontal Inf Orb	local efficiency	0.050	0.165	2.863	0.084
	L Frontal Med Orb	local efficiency	0.030	0.165	20.642	-0.457
	L Amygdala	betweenness centrality	0.027	0.319	12.015	-0.163
HC						
	NA	NA	NA	NA	NA	NA

Table 4.

Graph theory metric predictors of treatment response, determined with Spearman correlations between baseline graph theory metric and improvement in clinical assessment score (pretreatment minus post-treatment scores). Correlations were performed on aggregated patients (All PT), and with patients split by treatment cohort. *P*-values reported are uncorrected and from Spearman correlations. False discovery rate corrected *p*-values (*q*-value) are determined with $n=12$ (number of regions of interest). Negative rho indicates that greater nodal metrics correlate with lesser clinical improvement. Abbreviations) CBT: cognitive behavioral therapy, SSRI: selective serotonin reuptake inhibitor, HAMA: Hamilton anxiety rating scale, HAMD: Hamilton depression rating scale, DASS: depression, anxiety and stress scale.

cohort	region	metric	clinical assessment	p-value	q-value	rho
All PT	NA	NA	NA	NA	NA	NA
SSRI	R Frontal Sup Orb	betweenness centrality	HAMA	0.011	1.128	0.731
CBT	R Frontal Inf Orb	strength	HAMA	0.006	0.071	-0.716
	L Frontal Med Orb	local efficiency	DASS	0.09	0.158	-0.576
	L Hippocampus	local efficiency	DASS	0.005	0.055	-0.73
	R Hippocampus	local efficiency	DASS	0.037	0.158	-0.581

Table 5.

Graph theory metric correlates of treatment response as determined with Spearman correlations between change in nodal metric (determined by post-treatment minus baseline values) and improvement in clinical assessment score (pretreatment minus post-treatment scores). Correlations were performed on metrics that were found to significantly change with treatment by permutation test ($p < 0.05$). P -values from correlations are reported uncorrected (p) and false discovery rate corrected (q) with $n=7$ (total number of correlations performed). Abbreviations) CBT: cognitive behavioral therapy, SSRI: selective serotonin reuptake inhibitor, HAMA: Hamilton anxiety rating scale, HAMD: Hamilton depression rating scale, DASS: depression, anxiety and stress scale.

cohort	region	metric	clinical assessment	p-value	q-value	rho
All PT						
	NA	NA	NA	NA	NA	NA
SSRI						
	NA	NA	NA	NA	NA	NA
CBT						
	L Frontal Sup Orb	clustering coefficient	DASS	0.008	0.084	0.694
	L Frontal Med Orb	clustering coefficient	DASS	0.042	0.084	0.57
	L Frontal Med Orb	local efficiency	DASS	0.019	0.075	0.639